International Symposium
On Turbulence and Shear Flow
Phenomena (TSFP-8)
August 28 - 30, 2013 Poitiers, France

GRADIENT TRAJECTORY ANALYSIS OF THE TURBULENT/NON-TURBULENT INTERFACE IN A JET FLOW

Markus Gampert, Philip Schaefer, Jonas Boschung, Norbert Peters
Institute for Combustion Technology
RWTH-Aachen University
Templergraben 64, Aachen, Germany
m.gampert@itv.rwth-aachen.de

ABSTRACT

Based on planar high-speed Rayleigh scattering measurements of the mixture fraction Z of propane discharging from a turbulent round jet into co-flowing carbon dioxide at nozzle based Reynolds numbers Re_0=3,000-8,600, we use scalar gradient trajectories to investigate the local structure of the turbulent scalar field with a focus on the scalar turbulent/non-turbulent interface. The latter is located between the fully turbulent part of the jet and the outer flow. Using scalar gradient trajectories, we partition the turbulent scalar field into these three regions according to an approach developed by Mellado *et al.* (2009). Based on these different regions, we investigate in a next step zonal statistics of the scalar pdf $P(Z)$ as well as the scalar difference along the trajectory ΔZ and its mean scalar value Z_m, where the latter two quantites are used to parameterize the scalar profile along gradient trajectories. We show that the scalar probability density function $P(Z)$ can be reconstructed from zonal gradient trajectory statistics of the joint probability density function $P(Z_m,\Delta Z)$. Furthermore, we relate our results for the scalar turbulent/non-turbulent interface on the one hand to the findings made in other experimental and numerical studies of the turbulent/non-turbulent interface and discuss them on the other hand in the context of the flamelet approach and the modelling of probability density functions in turbulent non-premixed combustion.

1 Introduction

Turbulent mixing is a subject of immense interest owing to its occurence in numerous engineering applications, which involve the mixing of a scalar in a turbulent flow field. In a two-feed system, the state of mixing can be uniquely defined by a parameter called the mixture fraction Z, which is defined as the mass fraction of fuel stream in a given fuel-air mixture

$$Z = \frac{m_f}{m_f + m_{air}}, \tag{1}$$

where the subscripts f and air refer to fuel stream and air, respectively. According to this definition, Z varies between $Z = 0$ and $Z = 1$. Combustion occurs when the fuel mass fraction in a fuel/oxidizer mixture reaches a particular value, called the stoichiometric mixture fraction Z_{st}. The value of Z_{st} is about 0.06 for different hydrocarbon/air mixtures; for instance, for a propane-air mixture $Z_{st} = 0.06095$. Owing to the low values of stoichiometric mixture fraction, combustion occurs at the outer boundary of a turbulent fuel jet, which is characterized by turbulent regions adjacent to non-turbulent ones. When experimental investigations are performed, for instance, at the edge of a turbulent jet flow, the signal varies abruptly between a turbulent and a non-turbulent character for measurements of scalar quantities. Corrsin & Kistler (1955) first termed the layer at the outer edge of this turbulent/non-turbulent (T/NT) interface the laminar superlayer. We are considering a scalar quantity only, so that we will refer to the region in which the scalar signal changes from a turbulent to a laminar character in the following as the scalar T/NT interface to point out that all analyses is conducted in a scalar field.

Detailed spatial analyses of this region have been carried out experimentally (e.g. Holzner *et al.* (2007); Westerweel *et al.* (2009)) and numerically (e.g. da Silva & Taveira (2010); da Silva & Pereira (2011)) giving deeper insight into the vorticity dynamics close to the T/NT interface. In a previous work, cf. Gampert *et al.* (2012*a*), the contribution of the T/NT interface to the mixture fraction probability density function (pdf) P(Z) at various axial and radial locations has been examined. Then statistics such as the pdf of the location of the T/NT interface interface and the scalar profile across the latter were investigated and found to be in good agreement with literature data, cf. Westerweel *et al.* (2009). In addition, the scaling of the thickness δ of the scalar T/NT interface was analyzed at Reynolds numbers $Re_\lambda = 60-140$, where Re_λ denotes the local Reynolds number based on the Taylor scale λ, using the mixture fraction profile in interface normal direction. It was observed that $\delta/L \propto Re_\lambda^{-1}$, where L is an integral length scale, meaning that $\delta \propto \lambda$ - a finding that is in good agreement with dimensional scaling arguments postulated by da Silva & Taveira (2010).

The region of the T/NT interface was recently further analyzed by Mellado *et al.* (2009). In this work, the latter authors investigate the DNS of a temporally evolving shear layer using gradient trajectories. Mellado *et al.* (2009) applied this analysis to partition the scalar field into a fully turbulent zone, a zone containing the T/NT interface and the outer laminar flow. Based on the different regions, they examine the probability of these three zones at different locations in the shear layer and investigate the scalar probability density function and the conditional scalar dissipation rate in the zones in the presence of external intermittency.

To this end scalar gradient trajectories are calculated

from each grid point in ascending and descending direction until a local extremum is reached at which the scalar gradient vanishes and the Hessian is either positive-definite (minimum) or negative-definite (maximum). We define the local direction **n** of a gradient trajectory as

$$\mathbf{n} = \frac{\nabla Z}{|\nabla Z|}, \tag{2}$$

which is followed until the trajectory hits an extreme point.

The present study continues the investigation of the scalar T/NT interface in a turbulent jet flow and analyses the scalar pdf conditioned on the different regions of the flow field using gradient trajectories. To this end, we perform high frequency planar Rayleigh scattering measurements of pure propane C_3H_8 discharging from a free round jet into coflowing pure CO_2. In this case, the local mass fraction $Y_{C_3H_8}$ of propane is equal to the mixture fraction Z

$$Z = Y_{C_3H_8} = \frac{X_{C_3H_8} W_{C_3H_8}}{X_{C_3H_8}(W_{C_3H_8} - W_{CO_2}) + W_{CO_2}}. \tag{3}$$

In eq. (3), $X_{C_3H_8}$ is the propane mole fraction and $W_{C_3H_8}$ and W_{CO_2} are the molecular weights of propane and carbon dioxide, respectively. In section 2, we describe the experimental arrangement together with the calculation of scalar gradient trajectories, present the results for the zonal statistics in chapter 3 and conclude our paper in section 4.

2 Experiment

The measurement technique and the data post-processing have been described and validated in companion papers, cf. Gampert *et al.* (2013, 2012*c*), so that only a brief description is given in the following.

The experiments were performed in a co-flowing turbulent jet facility. Figure 1 shows the schematic of the experimental setup. The facility consists of a center tube made of steel with an inner diameter of 12 mm. The surrounding co-flow tube had a diameter of 150 mm and a length of 450 mm, which was large enough to reduce the experimental setup to a two-stream problem. In the latter tube a honeycomb is installed in the lower third to guarantee a uniform velocity profile.

Research grade propane (99.95% pure) was fed through the center tube using a flow controller (OMEGA FMA-2600A) at various flow rates to achieve the desired Reynolds number. The co-flow gas was chosen as carbon dioxide owing to its larger Rayleigh cross-section. For the different experimental runs, the mean velocity of CO_2 was 0.05 m/s. Table 1 shows the flow configurations of all the experimental runs made in this work. The Reynolds number Re_D based on jet exit conditions, was varied between 3,000 and 8,610 and the corresponding jet exit velocity was between 1.15 and 3.3 m/s. Furthermore, Re_λ $(= u_{rms}\lambda_u/\nu_{Cl})$ is the local Taylor based Reynolds number on the center line. For the calculation of this quantity, u_{rms} has been measured using Laser Doppler Anemometry (LDA), the kinematic viscosity on the centerline ν_{Cl} has been determined using the local concentration of the two gases, while the Taylor length $\lambda_u (= (15 u_{rms}\nu_{Cl}/\varepsilon)^{1/2})$ of the velocity field has been computed using an approximation formula, see Friehe *et al.* (1971).

For the Rayleigh scattering imaging, two frequency doubled beams ($\lambda_f = 527nm$) from a high-frequency dual-head Nd:YLF laser (Litron Lasers LDY303HE-PIV) were combined to deliver an energy of about 32 mJ/p at 1 kHz (32 W). To account for energy fluctuations, the signal is corrected on a shot by shot basis by a 12bit energy monitor (LaVision Online Energy Monitor). The polarization of both of the beams was normal to the jet axis which maximized the Rayleigh scattering signals from the radial-azimuthal plane. The beams were transformed into a horizontal collimated sheet using a combination of a Galilean telescope (expansion ratio of 1.5) and a cylindrical lens. The width and the thickness (FWHM) of the resultant sheet were approximately $10mm$ and $0.3mm$ respectively. Images were acquired at 1 kHz using a high-speed CMOS camera (LaVision HighSpeedStar 6) fitted with a camera lens (Nikon f.l. = 85 mm) stopped at $f/1.4$. An extension ring of 20 mm length was placed between the camera and the lens to minimize the working distance; the resulting field of view is about $60mm \times 60mm$. The signal-to noise ratio (SNR) in the pure propane region of the raw images was over 40. The time interval between the successive images

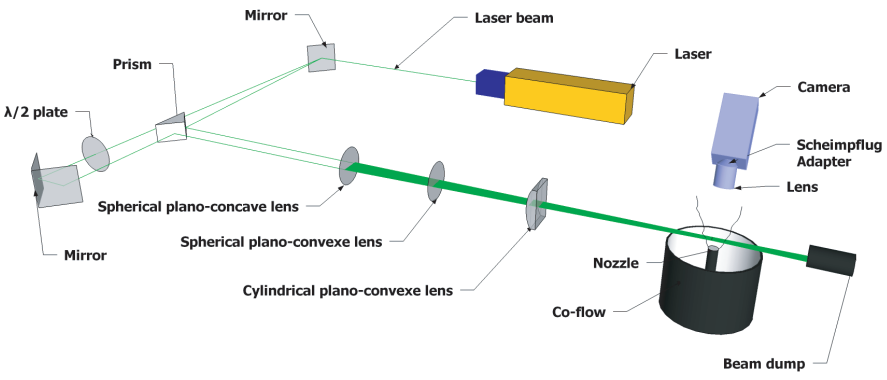

Figure 1. Experimental setup for the high-speed Rayleigh scattering measurements.

Table 1. Experimental parameters.

$\mathbf{x/d}$	10	15	20	30
Jet exit velocity $\mathbf{U_0}$ $[\mathbf{m/s}]$	1.15	1.76	1.82	3.30
Mean centerline velocity $\mathbf{U_{Cl}}$ $[\mathbf{m/s}]$	0.57	0.61	0.50	0.62
Nozzle based Reynolds number $\mathbf{Re_0}$	3,000	4,500	4,750	8,610
Taylor based Reynolds number $\mathbf{Re_\lambda}$	61	72	71	96

was $1ms$, while the in-plane resolution was 100 microns. This resolution is of the order of the Kolmogorov scale η, thus allowing a detailed investigation of gradient trajectories.

The major sources of systematic uncertainties are the departure from linearity of the camera response and the presence of noise in both propane and CO_2 streams. The departure from the linearity of the camera response is within 4%, as quoted by the manufacturer. The image noise was minimized using an optimal filter designed for the propane stream. However, there is residual noise left in the CO_2, after applying the optimal filter, which induces uncertainty in the calculation of the scalar gradients. The combined uncertainty arising from these sources is estimated to be below 5%. In a next step, the recorded time series of the plane at a fixed downstream location x/d is transformed into a spatial signal in streamwise direction with $\Delta x = U \cdot \Delta t$ based on Taylor's hypothesis. Hence, we obtain a frozen three-dimensional mixture fraction field.

The camera resolves a plane of 1024×1024 pixels at a frequency of 1kHz. This bounds the jet exit velocity U_0 to a value, at which the resolution in x-direction remains at the order of the Kolmogorov scale at the various downstream positions x/d. Note, that the analysis of the mixture fraction volume has been restricted in radial direction to $\tilde{r}(= r/(x - x_0)) < 0.1$, where x_0 denotes the virtual origin of the jet and has been found to be $x_0/d = -1.75$ and is performed at each axial location using three statistically independent sets of $5,400$ consecutive images.

3 Zonal statistics based on gradient trajectories

As described in section 1, we will in the following examine the mixture fraction fields based on the procedure developed by Mellado *et al.* (2009) using gradient trajectories. To this end, the flow is partitioned into three different regions using the statistics of scalar gradient trajectories - namely a fully turbulent zone, an outer flow region and embedded within these two the scalar T/NT interface.

In the following, gradient trajectories together with scalar minimum and maximum points are used to detect the different regions of the scalar field, see fig. 2 for an illustration: If a gradient trajectory associated with one specific grid point connects one minimum and one maximum point, this point is considered to be inside the fully turbulent zone. On the contrary, if the trajectory connects a maximum with the outer stream, where the mixture fraction is $Z = 0$ that point belongs to the scalar T/NT interface. Finally, all points whose trajectories do not reach an extreme point are considered to be in the outer flow. The approach has already been successfully applied in Gampert *et al.* (2012*c*), where it has been used to study profiles of the zonal probability of the three different regions over the non-dimensional radial coordinate $\tilde{r}$. It has been found that for $\tilde{r} < 0.08$ the scalar field is dominated by the fully turbulent region with an increasing contribution of the scalar T/NT interface, which is already present on the centerline with a zonal probability of approximately 0.05. For $\tilde{r} > 0.18$ in contrast, it is most probable to find the outer flow, whose contribution is not negligible starting at $\tilde{r} < 0.06$. In between, however, the structure of the scalar field is mainly dominated by the scalar T/NT interface. In the present study, we will investigate in particular the zonal statistics of the scalar pdf $P(Z)$ in the different regions in more detail.

Let us note that this partitioning is based on non-local information, as the grid points at a given radial distance from the centerline with a scalar value between the free-stream and the centerline value might belong to the scalar T/NT interface and the distinction is only possible by following the corresponding trajectory. Mellado *et al.* (2009) showed that this non-local approach allows to detect engulfed regions, which is not possible if the interface definition is based on a single-valued envelope surface. However, an outer limit to the interface is also set by a threshold in the magnitude of the scalar gradient, below which the scalar is approximately a homogenous field with the outer flow value $Z = 0$. This second criterion defines the conventional intermittency function and separates the non-turbulent zones from the scalar T/NT interface.

This differentiation between the outer non-turbulent zones and the T/NT interface has been introduced for several reasons. First, it is needed from the numerical point of view because the gradient approaches zero as one moves towards the outer homogeneous region so that below a threshold there is only noise, and the gradient direction is numerically undetermined. Second, this distinction is the conventional one used to define the intermittency factor and can be used to compare with traditional results using only this quantity. Finally, it is also useful to simplify possible models, since the pdf of the scalar field in these non-turbulent regions is just a delta function at the outer flow value $Z = 0$ and the scalar dissipation can be approximated by zero. In summary, a point at a given distance r from the centerline can be part of the non-turbulent outer flow, belong to the scalar T/NT interface or be located within a turbulent region.

In a first step, we calculate the extreme points in the experimentally obtained three-dimensional mixture fraction field as well as the corresponding gradient trajectories using the same numerical procedures already applied for instance in Gampert *et al.* (2011, 2012*b*); Schaefer *et al.* (2010) so that we can afterwards define the different regions in the scalar field.

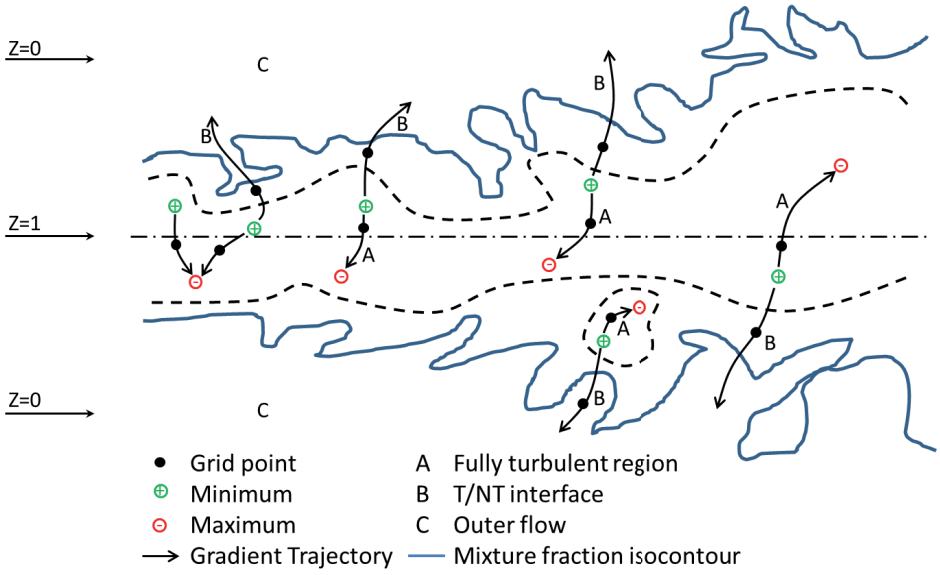

Figure 2. Flow partitioning based on gradient trajectories: A, trajectory from minimum to maximum, fully turbulent zone; B, from outer flow to maximum, turbulent interface; C, outer flow.

A parametrization of the scalar field along a gradient trajectory is necessary for a statistical investigation. To this end, Peters & Trouillet (2002) propose to use the arithmetic mean $Z_m = (Z_{max} + Z_{min})/2$ of the minimum and maximum value of the extremal points that bound the gradient trajectory as well as the scalar difference $\Delta Z = Z_{max} - Z_{min}$.

Computing for each grid point in the experimentally obtained mixture fraction field the corresponding gradient trajectories, we can in a first step calculate the joint probability density function (jpdf) $P(Z_m, \Delta Z)$ for the overall domain. As is shown in fig. 3, we obtain a triangular shaped jpdf, which has a distinct maximum at around $Z_m = 0.30$, $\Delta Z = 0.15$. The theoretical boundaries of this jpdf are given by $Z_m = \Delta Z/2$ and $Z_m + \Delta Z/2 = 0.6$, as $Z = 0.6$ is the maximum mixture fraction value.

Based on the method described above, we distinguish for this jpdf the fully turbulent $P_t(Z_m, \Delta Z)$ and the interface region $P_s(Z_m, \Delta Z)$. The resulting jpdfs are shown in fig. 4 (a) for the scalar T/NT interface and in (b) for the turbulent region. We observe in fig. 4(a) that all values of this jpdf are concentrated around $Z_m = \Delta Z/2$ as the criterion for the interface detection is that the trajectory connects the outer flow ($Z = 0$) with a maximum point so that $Z_m = (Z_{max} + Z_{min})/2 = Z_{max}/2$ and $\Delta Z = Z_{max} - Z_{min} = Z_{max}$. However, though the jpdf in the T/NT interface should only be represented by a line defined by $Z_m = \Delta Z/2$, it has a thin distinct width which is limited by the above mentioned residual noise level after post-processing. Furthermore, it has a maximal probability at $Z_m = 0.16$ and $\Delta Z = 0.32$ from which we find a decreasing probability towards the origin and the longest trajectories for which $Z_m = 0.29$ and $\Delta Z = 0.58$. From fig. 4(b) which shows the jpdf $P_t(Z_m, \Delta Z)$ in the fully turbulent region, it is obvious that the rest of the total jpdf, cf. fig 3, corresponds to the turbulent part. As the total jpdf, it has a triangular shape with a maximum at around $Z_m = 0.1 - 0.2$, $\Delta Z = 0.30$ with a cropped off lower

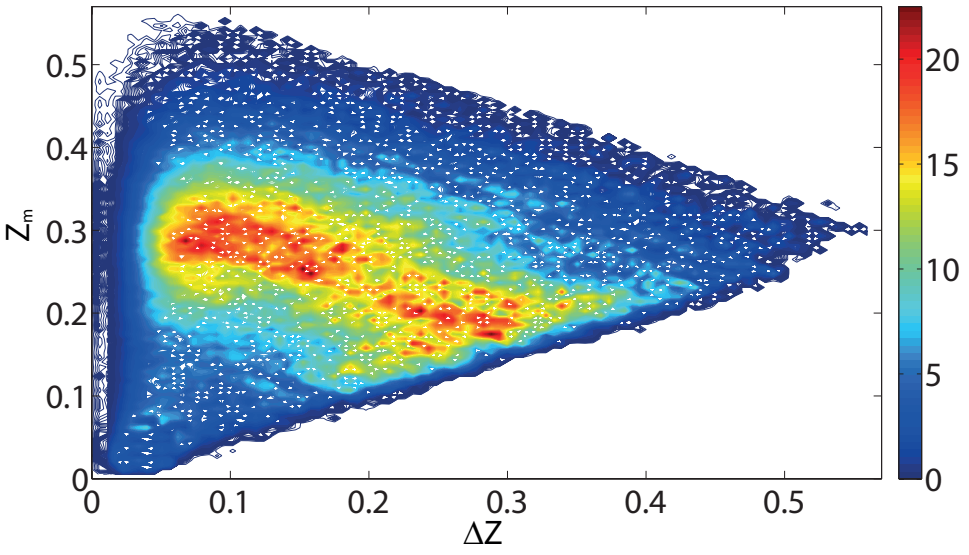

Figure 3. Isocontour lines of the jpdf $P(Z_m, \Delta Z)$ for the whole domain within $\tilde{r} < 0.1$ obtained at $x/d = 15$.

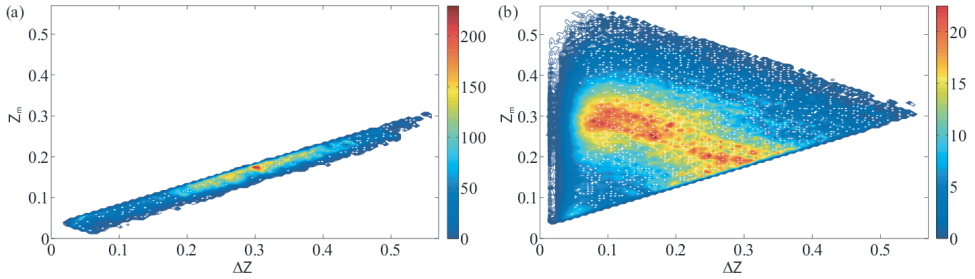

Figure 4. Isocontour lines of the jpdfs (a) $P_s(Z_m,\Delta Z)$ for the the T/NT interface region and (b) $P_t(Z_m,\Delta Z)$ for the fully turbulent part of the domain within $\tilde{r} < 0.1$ obtained at $x/d = 15$.

edge due to the missing T/NT interface contributions. Naturally, the jpdf in the outer flow has a peak at $Z_m = \Delta Z = 0$.

Based on the jpdf of these two parameters, cf. figs. 3 and 4, we will in the following investigate the scalar pdf $P(Z)$ in the different regions of the field and show that it can be reproduced from $P(Z_m,\Delta Z)$ obtained by gradient trajectory statistics. In a first step, we therefore write the overall pdf in terms of its different contributions

$$P(Z) = \gamma[(1-s)P_t(Z) + sP_s(Z)] + (1-\gamma)P_o(Z), \quad (4)$$

where γ is the intermittency factor defined as the fraction of the signal that is not due to the outer flow and s is the interface contribution, given by the fraction of the T/NT interface within the remaining part. Furthermore, $P_t(Z)$ is the scalar pdf in the fully turbulent zone, $P_s(Z)$ denotes the pdf stemming from the T/NT interface and $P_o(Z)$ is the scalar pdf in the outer flow, which by definition is a delta peak at zero. Each of these pdfs as well as the overall one can be calculated purely from the jpdf of the introduced gradient trajectory parameters by Peters & Trouillet (2002)

$$P_i(Z) = \int_0^1 \int_0^{\Delta Z_{max}} P_l(Z;Z_m,\Delta Z) P_i(Z_m,\Delta Z) d\Delta Z dZ_m. \quad (5)$$

In eq. (5), $P_i(Z_m,\Delta Z)$ is the zonal jpdf of Z_m and ΔZ, while $P_l(Z)$ is the local distribution function of Z within the gradient trajectory of length l. However, as the latter is unknown, we follow the approximation of Peters & Trouillet (2002), who assume a sine function for the profile of Z

$$Z = Z_m + \frac{\Delta Z}{2}\sin(\pi\tilde{s} - \pi/2), \quad (6)$$

where $\tilde{s} = s/l$ is a normalized coordinate along the trajectory which increases linearly from zero to one. Using such a scalar profile, we obtain

$$P_l(Z;Z_m,\Delta Z) = \frac{P(s)}{|\,\partial Z/\partial s\,|} \quad (7)$$

that can be computed for each combination $(Z_m,\Delta Z)$ following Peters & Trouillet (2002)

$$P_l(Z;Z_m,\Delta Z) = \frac{\pi^{-1}}{|\,(Z-Z_m+\Delta Z/2)^{1/2}(Z_m+\Delta Z/2-Z)^{1/2}\,|}. \quad (8)$$

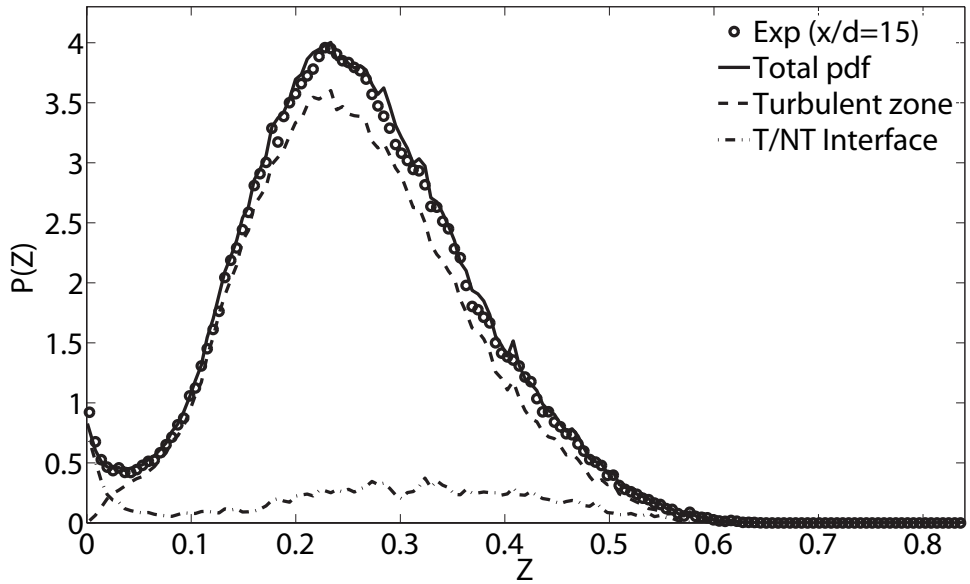

Figure 5. Comparison of the measured pdf $P(Z)$ obtained at $x/d = 15$ with the one calculated from eq. (4). In addition, the weighted zonal pdfs of the fully turbulent $\gamma[(1-s)P_t(Z)]$ and of the scalar T/NT interface $\gamma[sP_s(Z)]$ are shown.

Introducing eq. (7) in eq. (5) together with the jpdfs shown in figs. 3 and 4 allows us to reconstruct the scalar pdfs within the different zones of the scalar field, see fig. 5 that is calculated from the data obtained at $x/d = 15$. We observe for the experimentally obtained pdf (open circles) a bimodal shape with a maximum at $Z = 0.23$, a non-zero value at the origin of $P(Z = 0)$ close to unity and and intermittency factor $\gamma = 0.995$. In addition, the scalar pdfs computed separately for the turbulent and the interface parts are shown weighted by its respective prefactors according to eq. (4) together with the reconstructed overall pdf, which is also calculated according to eq. (4) (note that the pdf of the outer flow region P_o is not shown in fig. 5 as it is only a delta peak at the origin). Nevertheless, it is included in the total pdf to which it only has a very small contribution ($1-\gamma = 0.005$). We observe a very good qualitative and quantitative agreement of the reconstructed pdf with the measured one, further validating that the ansatz (eq. (6)) is in close agreement with the real scalar profile along the rajectories. Furthermore, we can attribute specific parts of the measured pdf to different flow regions. In the fully turbulent part, the pdf is close to Gaussian shape with a value of $P(Z = 0) = 0$ at the origin and a maximum at $Z = 0.23$, the location of which coincides with the one of the total pdf. In contrast, the pdf of the T/NT interface recovers the non-zero value of the measured pdf at the origin, which is not only due to contributions from the outer flow. In addition, it has a non-zero value over the whole range of mixture fraction values with a small maximum at approximately $Z = 0.33$. This may be explained by the fact that the T/NT interface contains not only the T/NT interface itself but also the adjacent regions up to the first maximum point. Finally its contribution s calculated from the fraction of the interface region within the non-outer flow part is $s = 0.107$.

4 Conclusion

We have presented planar high-speed Rayleigh scattering measurements of the mixture fraction Z of propane discharging from a turbulent round jet into co-flowing carbon dioxide at nozzle based Reynolds numbers Re_0=3,000-8,600, based on which we have investigated the local structure of the turbulent scalar field as well as the scalar pdf using scalar gradient trajectories.

The latter have been calculated for every grid point and scalar profiles along the latter are parametrized by the arithmetic mean Z_m of minimum and maximum value of the extremal points that bound the gradient trajectory and the scalar difference ΔZ between them. Using these parameters, we have partitioned the turbulent scalar field into three regions - a fully turbulent one, where each trajectory connects a minimum and a maximum point, the outer flow with $Z = 0$ and a meandering scalar T/NT interface, where a maximum point is connected with the outer flow via a gradient trajectory - the latter structure is embedded within the former two. In a next step, we have investigated the jpdf $P(Z_m, \Delta Z)$ as well as the marginal pdfs $P(Z_m)$ and $P(\Delta Z)$ in the different zones and observe distinct characteristics for each of them: many small fluctuations together with a large mean scalar value are typical for the fully turbulent region, while the regularly observed large jump of the scalar value is caught by the gradient trajectory statistics in the scalar T/NT interface. As the latter start in the outer flow at $Z = 0$, it also directly follows from this large jump that the T/NT interface trajectories frequently contain the comparitively small value of stroichiometric mixture Z_{st}.

Finally, we have presented a method to reconstruct the overall scalar pdf $P(Z)$ based on gradient trajectory statistics using the jpdf $P(Z_m, \Delta Z)$ in the different zones of the scalar field. We observe a good agreement between the experimentally obtained pdf with the reconstructed one, where $P_t(Z)$ in the turbulent part has the shape of a Gaussian-bell curve, while $P_s(Z)$ in the T/NT interface has a non-zero value at the origin from which it decreases to zero.

REFERENCES

Corrsin, S. & Kistler, A. L. 1955 Free-stream boundaries of turbulent flows. *NACA Report* **1244**.

da Silva, C. B. & Pereira, J. C. 2011 The role of coherent vortices near the turbulent/non-turbulent interface in a planar jet. *Phil. Trans. R. Soc. A* **369**, 738–753.

da Silva, C. B. & Taveira, R. R. 2010 The thickness of the turbulent/nonturbulent interface is equal to the radius of the large vorticity structures near the edge of the shear layer. *Phys. Fluids* **22**, 121702.

Friehe, C. A., Van Atta, C. W. & Gibson, C. H. 1971 Jet turbulence dissipation rate measurements and correlations. *AGARD Turbulent Shear Flows* **CP-93**, 18.1–18.7.

Gampert, M., Goebbert, J. H., Schaefer, P., Gauding, M., Peters, N., Aldudak, F. & Oberlack, M. 2011 Extensive strain along gradient trajectories in the turbulent kinetic energy field. *New J. Phys.* **13**, 043012.

Gampert, M., Narayanaswamy, V., Schaefer, P. & Peters, N. 2012*a* Conditional statistics of the turbulent/non-turbulent influence in a jet flow. *submitted to J. Fluid Mech.* .

Gampert, M., Schaefer, P., Goebbert, J.H. & Peters, N. 2012*b* Decomposition of the field of the turbulent kinetic energy into regions of compressive and extensive strain. *Physica Scripta T* **in press**.

Gampert, M., Schaefer, P., Narayanaswamy, V. & Peters, N. 2012*c* Gradient trajectory analysis in a jet flow for turbulent combustion modelling. *J. Turbulence* .

Gampert, M., Schaefer, P. & Peters, N. 2013 Experimental investigation of dissipation element statistics in scalar fields of a jet flow. *accepted for publication in J. Fluid Mech.* .

Holzner, M., Luethi, B., Tsinober, A. & Kinzelbach, W. 2007 Acceleration, pressure and related quantities in the proximity of the turbulent/non-turbulent interface. *J. Fluid Mech.* **639**, 153–165.

Mellado, J. P., Wang, L. & Peters, N. 2009 Gradient trajectory analysis of a scalar field with internal intermittency. *J. Fluid Mech.* **626**, 333–365.

Peters, N. & Trouillet, P. 2002 On the role of quasi-one-dimensional dissipation layers in turbulent scalar mixing. In *Annual Research Briefs*, pp. 27–40. Center for Turbulence Research, Stanford University.

Schaefer, P., Gampert, M., Goebbert, J. H., Wang, L. & Peters, N. 2010 Testing of different model equations for the mean dissipation using Kolmogorov flows. *Flow Turb. Comb.* **85**, 225–243.

Westerweel, J., Fukushima, C., Pedersen, J.M. & Hunt, J.C.R. 2009 Momentum and scalar transport at the turbulent/non-turbulent interface of a jet. *J. Fluid Mech.* **631**, 199–230.